American Mineralogist, Volume 92, pages 713–721, 2007

Single-crystal FTIR and X-ray study of vishnevite, ideally $[Na_6(SO_4)][Na_2(H_2O)_2](Si_6Al_6O_{24})$

Giancarlo Della Ventura,[1,*] Fabio Bellatreccia,[1] Gian Carlo Parodi,[2] Fernando Cámara,[3] and Massimo Piccinini[1,4]

[1]Dipartimento di Scienze Geologiche, Università Roma Tre, Largo S. Leonardo Murialdo 1, I-00146 Roma, Italy
[2]Laboratoire de Minéralogie, Museum National d'Histoire Naturelle, 61, rue Buffon, F-75005 Paris
[3]CNR-Istituto di Geoscienze e Georisorse, unità di Pavia, via Ferrata 1, I-27100 Pavia, Italy
[4]I.N.F.N., Laboratori Nazionali di Frascati, Via E. Fermi, 40, I-00044 Frascati (Rome), Italy

Abstract

This paper reports a single-crystal FTIR spectroscopic study of vishnevite, ideally $[Na_6(SO_4)][Na_2(H_2O)_2](Si_6Al_6O_{24})$, a member of the cancrinite group of feldspathoids. The study was done on several crystals from various geological occurrences. Infrared spectra show that most samples, and in particular the specimens from the holotype locality at Vishnevye Mountains (Urals, Russia), contain molecular CO_2 as the main carbon species in the structural pores, while the specimens from Loch Borolan (Scotland) were found to be CO_3-rich. Polarized-light measurements show that the linear CO_2 molecules are oriented perpendicular to the crystallographic **c** axis. Structure refinement of sample Pi4 from Latium (Italy) shows usual $H_2O\cdots Na\cdots H_2O$ sequences within the undecahedral cages; however, difference Fourier maps suggest the presence of additional protons in the channels, possibly forming OH groups. The FTIR spectra show three absorptions in the 3800–3200 cm^{-1} region. The first one, at 3590 cm^{-1} is strongly polarized for $\mathbf{E}\perp\mathbf{c}$ while the second, at 3535 cm^{-1}, behaves almost isotropic. These two bands are assigned to the stretching vibrations of an asymmetric water molecule in the structural cages. The third broad absorption at 3320 cm^{-1}, is predominantly polarized for $\mathbf{E}\|\mathbf{c}$ and is assigned to additional OH groups in the channels. Detailed microspectroscopic mapping showed several samples from Latium (Italy) to be zoned with respect to the CO_2/CO_3 content, thus pointing to a possible use of the volatile content of these minerals for petrological modeling.

Keywords: Vishnevite, EMPA, crystal structure refinement, FTIR spectroscopy, channel molecules

Introduction

Vishnevite, $[Na_6(SO_4)][Na_2(H_2O)_2](Si_6Al_6O_{24})$, is a relatively rare member of the cancrinite group, first found at Vishnevye Gory, Urals, Russia (Beliankin 1944) and later in a few other occurrences (see Deer et al. 2004 for a compilation). Cancrinite minerals are feldspathoids characterized by hexagonal rings of (Si, Al) tetrahedral layers stacked along [001] so as to form a three dimensional framework. Different stacking sequences are possible, and these give rise to a large variety of species. An updated list can be found in Bonaccorsi and Merlino (2005). The simple ABAB... sequence (where A and B are the position of the first and second layer in the sequence, following the nomenclature of the closest-packed structures) is common to several natural (nine up to present) and synthetic phases in this group. These AB phases can be further classified into two series: the cancrinite-vishnevite series and the davyne-microsommite-quadridavyne series (cf. Bonaccorsi and Merlino 2005). Their framework is characterized by open 12-ring channels running along [001], and by columns of base-sharing undecahedral cages ($[6^612^{2/2}]$ and $[4^66^5]$ in the IUPAC nomenclature, respectively). In cancrinite-type minerals, the undecahedral cages contain sequences of alternating Na cations and water molecules, while the large channels are filled by carbonate groups in ideal cancrinite and by sulfate groups in ideal vishnevite (e.g., Bonaccorsi and Merlino 2005). There is a complete solid solution between cancrinite and vishnevite, with intermediate terms named sulfatic cancrinite or carbonatic vishnevite (Hassan and Grundy 1984). The substitution of SO_4^{2-} for CO_3^{2-} groups along the cancrinite-vishnevite series is correlated with the entry of significant amounts of K in the channels; when the (Na,Ca): K is nearly = 1, there is the possibility of long-range ordering of sulfate groups and extra-framework cations, such as in pitiglianoite, which is characterized by a threefold supercell with respect to cancrinite (Merlino et al. 1991; Bonaccorsi and Orlandi 1996).

Reliable and complete chemical analyses are difficult to obtain for these minerals, due to the presence of different types of extra-framework anions and cations. Recent spectroscopic work (Della Ventura and Bellatreccia 2004; Della Ventura et al. 2005) has shown that molecular CO_2 is also a common constituent in cancrinite group minerals. Therefore, it is important to not only determine the amount of carbon but also its speciation in the structure of these phases. Furthermore, Gesing and Buhl (2000) described a synthetic (HCO_3)-containing cancrinite [ideally $Na_{7.6}(Al_6Si_6O_{24})(HCO_3)_{1.2}(CO_3)_{0.2}(H_2O)_2$], thus pointing at the possible presence of a third type of carbon species in these microporous materials. One further problem relating to the crystal chemistry of these minerals is the possible simultaneous presence of H_2O and hydroxyl groups in the structural pores, again requiring characterization of the speciation of H in the sample. Basic cancrinite, for instance, is known to contain water molecules in the cages and hydroxyl groups in the large

* E-mail: dellaven@uniroma3.it

channels (Hassan and Grundy 1991) and sodalites with variable H_2O/OH contents have been described (Engelhardt et al. 1992; Wiebcke et al. 1992). In addition, the possible presence of H in the form of oxonium ions (H_3O^+) has been proposed for cancrinite (Galitskii et al. 1978).

IR spectroscopy is routinely used to characterize both the amount and the speciation of H and C in glasses (Ihinger et al. 1994; King et al. 2002). However, the application of this technique to the study of carbon in silicates has been limited to beryls (e.g., Aines and Rossman 1984), cordierite (e.g., Armbruster and Bloss 1980; Khomenko and Langer 2005), and phyllosilicates (Zhang et al. 2005).

We present here a spectroscopic study of several vishnevite samples and confirm that, in addition to diffraction experiments, FTIR methods are extremely useful in characterizing the presence, speciation, and the orientation of extra-framework molecules in these feldspathoids.

Samples and experimental methods

Table 1 gives a list of the samples examined in this study. Some of these samples were provided by mineral collectors active in the Latium area, whereas others were obtained from the collection of the Museum of Mineralogy of the University of Roma "La Sapienza" (MMUR) or from the Museum of Mineralogy of the École des Mines, Paris. The analyzed crystals were identified by powder or single-crystal X-ray diffraction and powder FTIR spectroscopy; this latter technique is in fact well known as a means to unambiguously identify the various cancrinite-group minerals based on the low-frequency 1200–500 cm^{-1} region (Ballirano et al. 1996; Della Ventura and Bellatreccia 2004; Cámara et al. 2005).

Microprobe analyses were done using a CAMEBAX 50X WDS-microprobe, at Camparis, Université Paris VI. Operating conditions were 15 kV accelerating voltage and 15 nA beam current, with a beam size of 10 μm; counting time was 10 s on both peak and background. Standards, spectral lines, and crystals used were: wollastonite (Si*K*α, TAP; Ca*K*α, PET), corundum (Al*K*α, TAP), jadeite (Na*K*α, TAP), orthoclase (K*K*α, PET), magnetite (Fe*K*α, LIF), barite (S*K*α, PET), sylvite (Cl*K*α, PET), and fluorphlogopite (F*K*α, TAP). Data reduction was done by the PAP method (Pouchou and Pichoir 1985). Powder FTIR spectra were collected on a Nicolet Magna 760 spectrometer, equipped with a room-*T* DTGS detector and a KBr beamsplitter (4 cm^{-1} resolution, 32 scans averaged for each spectrum). Single-crystal micro-FTIR spectra were collected with a NicPlan microscope, equipped with a MCT-A liquid nitrogen-cooled detector and either a KBr beamsplitter for the MIR (medium infrared-red) region or a CaF_2 beamsplitter for the NIR (near infrared-red) region. Nominal resolution was 4 cm^{-1} and final spectra are the average of 128 scans. Samples were prepared as doubly polished chips; in some cases regularly shaped, cleavage fragments were used. For polarized measurements a gold wire-grid, ZnS substrate IR polarizer was used; the crystals were oriented using the external morphology as a guide, and the orientation was checked using a petrographic microscope.

A crystal of vishnevite from Pitigliano, sample Pi4 (Table 1) was examined with a Bruker AXS SMART Apex single-crystal diffractometer with a 4 cm crystal-to-detector distance under graphite-monochromatized Mo*K*α X-radiation at 55 kV and 30 mA. Miscellaneous information is summarized in Table 2. Three-dimensional data were integrated and corrected for Lorentz, polarization, and background effects using the SAINT+ software version 6.45a (Bruker AXS). Unit-cell dimensions (Table 2) were calculated from least-squares refinement of the position of all collected reflections. Frame widths of 0.3° in ω were used to collect 560 frames per batch in three batches at different φ values (0°, 90°, and 180°) collected at 2θ = –39°, respectively. Counting time per image was 10 s. A total of 13 292 reflections was collected in the θ range 1.9–37.9°, corresponding to 2581 unique reflections (R_{int} = 1.96%). Raw intensity data were corrected for absorption using SADABS ver. 2.03 program (Sheldrick 1996).

Microchemical data

Table 3 gives selected microprobe analyses and crystal-chemical formulae for the studied vishnevites. The Si:Al ratio apfu (atoms per formula unit) is very close to 1:1, except for sample Pi4, which shows slightly higher Si with respect to Al. The Ca content is almost negligible for all samples, while Na is dominant as the extra-framework cation. All samples contain appreciable K, and crystal Vish/4 from Vishnevye Gory is significantly rich in K (9.29 wt%), in agreement with previous data from the literature (Beliankin 1944). Carbon could not be quantified by EMP; however, the microchemical data show that SO_4 is the dominant anionic group in the structural pores. Sample Pi4 has SO_4 close to 1.0 apfu and can thus be classified as an end-member vishnevite. The crystal-chemical formulae were calculated according to Ballirano et al. (1995). The weight percent of CO_2, which was obtained as the amount necessary to saturate the O excess (Table 3), is relatively high (up to 2.59 wt%) for both samples from Scotland while it is almost negligible in all other samples. Despite the low analytical totals, probably due to some loss of alkali elements during the electron bombardment, the carbon contents calculated from the EMP data are in fairly good agreement with the spectroscopic data (see below).

Non-polarized single-crystal FTIR data

Basic considerations

A typical single-crystal non-polarized room-*T* FTIR spectrum of vishnevite, collected on a very thin fragment of a crystal from the holotype locality (Vishnevy Gory, Urals), is displayed in Figure 1 in the range 7500–650 cm^{-1}. It shows several absorption bands, which can be assigned as follows (Della Ventura et al. 2005):

(1) The broad and very strong absorption at around 1000 cm^{-1} that is actually composed of several overlapping bands, is assigned to stretching vibrations of tetrahedral T-O bonds; the sharp band at 1186 cm^{-1}, visible on the high-frequency side of the main band, can be assigned to stretching vibrations of SO_4 groups. The absorption of the tetrahedral framework is off-scale in the spectrum of Figure 1 due to the crystal thickness.

(2) The group of weak bands centered at around 2100 cm^{-1} is assigned to the first overtone of the stretching modes of the T-O and SO_4 absorptions.

(3) The very intense and sharp band at 1627 cm^{-1} is assigned to the ν_2 bending mode of the water molecule (cf. Ihinger et al. 1994).

(4) The very broad and intense absorption centered at around 3500 cm^{-1} is composed of at least three overlapping features at ~3590, 3530, and 3320 cm^{-1}, which are assigned to the stretch-

Table 1. Studied samples of vishnevite

Label	Occurrence	Notes
Pi4	Pitigliano, Tuscany (GR)	In miarolitic cavity, syenitic ejectum, associated with datolite, andraditic garnet, biotite, diopside and Fe-oxides
F3A	Farnese, Latium (VT)	In miarolitic cavity, syenitic ejectum, associated with farneseite, andraditic garnet, augite, biotite and sodalite
DD2	Farnese, Latium (VT)	In miarolitic cavity, syenitic ejectum, associated with augite, biotite and Fe-oxides
AH	Alban Hills, Latium (RM)	In miarolitic cavity, lava, associated with analcime, and olivine
Vish/4	Vishnevye Mt. (Urals, Russia)	From the MMUR collection, No. 28379/4
V35209	Vishnevye Mt. (Urals, Russia)	From the École des Mines collection, No. 35209
Vish/1	Loch Borolan (Scotland, GB)	From the MMUR collection, No. 24783/1
V72	Loch Borolan (Scotland, GB)	From the École des Mines collection, No. 50071/72

TABLE 2. Crystal data and structure refinement for vishnevite Pi4

Space group	$P6_3$
a (Å)	12.7228(3)
c (Å)	5.1980(3)
V (Å^3)	728.67(5)
Z	1
Wavelength (Å)	0.71073 (Mo$K\alpha$)
Crystal size (mm^3)	0.270 × 0.250 × 0.150
θ range for data collection (°)	1.85 to 37.91
Index ranges	$-21 \le h \le 21$; $-20 \le k \le 21$; $-8 \le l \le 8$
Reflections collected	13292
Independent reflections (%)	2581 [R(int) = 1.96]
Completeness to theta = 37.91°	99.1%
Absorption coefficient (mm^{-1})	1.05
Refinement method	Full-matrix least-squares on F^2
Data/restraints/parameters	2581/0/90
Goodness-of-fit on F^2	1.178
Final R indices [$I > 2\sigma(I)$] (%)	R = 3.26, wR^2 = 9.31
R indices (all data) (%)	R = 3.31, wR^2 = 9.36
Largest diff. peak and hole (e$^-$Å^{-3})	0.884 and –0.418

TABLE 3. Selected microprobe analyses (wt%) and crystal-chemical formulae for the studied vishnevite samples

Sample	Pi4	F3A	DD2	AH	Vish/4	V35209	Vish/1	V72
SiO_2	35.72	34.19	35.10	34.16	33.88	34.92	34.56	34.70
Al_2O_3	28.02	29.45	28.57	29.92	28.78	29.66	29.48	29.64
FeO	0.06	0.08	0.03	0.02	0.04	0.00	0.01	0.00
CaO	0.28	0.24	0.49	0.12	0.20	0.17	4.00	2.48
K_2O	3.15	6.56	4.30	3.57	9.29	0.79	0.38	0.64
Na_2O	20.03	18.34	19.11	21.05	15.67	21.37	20.18	21.41
SO_3	7.72	6.02	5.90	5.85	6.72	7.23	4.30	4.67
Cl	0.00	0.10	0.03	0.00	0.03	0.01	0.00	0.01
F	0.00	0.00	0.00	0.07	0.00	0.03	0.00	0.00
H_2O*	3.44	3.45	3.43	3.47	3.38	3.50	3.46	3.48
CO_2†	0.00	0.25	0.40	0.50	0.00	0.00	2.59	2.08
	98.42	98.68	97.37	98.73	97.99	97.68	98.96	99.11
–O = F,Cl	0.00	0.02	0.01	0.03	0.01	0.01	0.00	0.00
Total	98.42	98.66	97.36	98.70	97.98	97.67	98.96	99.11
Number of atoms on the basis of 12 (Si + Al) atoms per formula unit								
Si	6.24	5.95	6.12	5.90	6.00	6.00	5.98	5.98
Al	5.76	6.05	5.88	6.10	6.00	6.00	6.02	6.02
Sum	12.00	12.00	12.00	12.00	12.00	12.00	12.00	12.00
Ca	0.05	0.05	0.09	0.02	0.04	0.03	0.74	0.46
Fe^{2+}	0.01	0.01	0.01	0.00	0.01	0.00	0.00	0.00
K	0.70	1.46	0.96	0.79	2.10	0.17	0.08	0.14
Na	6.78	6.19	6.47	7.06	5.38	7.11	6.78	7.15
Sum	7.54	7.71	7.52	7.87	7.53	7.31	7.60	7.75
SO_4^{2-}	1.01	0.79	0.77	0.76	0.89	0.93	0.56	0.60
Cl^-	0.00	0.03	0.01	0.00	0.01	0.00	0.00	0.00
F^-	0.00	0.00	0.00	0.04	0.00	0.01	0.00	0.00
Sum	1.01	0.82	0.78	0.80	0.90	0.94	0.56	0.60
H_2O	2.00	2.00	2.00	2.00	2.00	2.00	2.00	2.00
CO_3^{2-}	0.00	0.06	0.10	0.12	0.00	0.00	0.61	0.49
O	23.91	24.06	24.09	24.12	23.88	23.73	24.61	24.49
O‡	23.91	24.00	24.00	24.00	23.88	23.73	24.00	24.00
Si/Al	1.08	0.99	1.04	0.97	1.00	1.00	0.99	0.99

* Calculated to give two water molecules pfu.
† Calculated according to Ballirano et al. (1995).
‡ Calculated after balancing with CO_3^{2-}.

ing modes of the water molecules or OH groups, as it will be discussed in more detail below.

(5) The band at 5218 cm^{-1} (see also inset in Fig. 1) is assigned to the $\nu_2 + \nu_3$ combination of the stretching and bending motions of the water molecule (Ihinger et al. 1994).

(6) The doublet at 7010–6700 cm^{-1} (inset in Fig. 1) is assigned to the first overtone of the stretching vibration of the water molecule (2 ν_3).

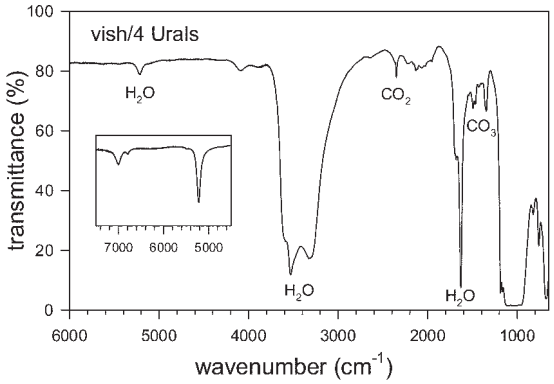

FIGURE 1. Single-crystal unpolarized-light spectrum of vishnevite Vish/4 from Vishnevy Gory, Urals. Spectrum collected on a randomly oriented very thin crystal fragment. The inset shows the 4500–7500 cm^{-1} NIR region collected on a thicker fragment.

(7) The very sharp band at 2351 cm^{-1} is the most notable feature of the spectrum of Figure 1. It is assigned to the ν_3 antisymmetric stretching mode of the $^{12}CO_2$ molecule (Della Ventura et al. 2005). Such absorption is very well known for glasses (see Ihinger et al. 1994 and King et al. 2002 for a complete list of references), while for minerals it has been reported in CO_2-bearing phases such as cordierite (Armbruster and Bloss 1980; Khomenko and Langer 2005) or beryl (Wood and Nassau 1967), or very recently, in other cancrinite-group minerals (farneseite: Cámara et al. 2005 and pitiglianoite: Della Ventura et al. 2005) where it occurs at a constant wavenumber of ~2350 cm^{-1}.

(8) The bands in the 1440–1500 cm^{-1} region are assigned to the ν_3 antisymmetric stretching vibrations of the CO_3 carbonate group (White 1974).

(9) The assignment of the two weak but well-defined bands at 4080 and 3870 cm^{-1} is still unclear. Their frequency is very close to combination modes involving the fundamental stretching of an O-H group coupled with the Si-O stretching in various forms of hydrous silica (e.g., Stone and Walrafen 1982).The possible assignment to the combination of an O-H stretching vibration with that of a metal-oxygen (e.g., Na-O) stretching has been proposed for Na-rich glasses (Ihinger et al. 1994). This point will be discussed in more details below.

In summary, the FTIR spectrum of a cancrinite-mineral, when collected in the whole NIR-MIR energy range, contains full information on the presence and speciation of H and C in the investigated crystal. Below we will describe in more detail the features observed for different samples and discuss the applications to the crystal-chemistry of vishnevite, as well as some possible applications to geological thermometry.

The C-O bands

Figure 2 shows the spectra measured in the 2600–1300 cm^{-1} range. In this region, the most prominent feature is the intense absorption centered around 1600 cm^{-1} due to the ν_2 bending mode of H_2O. The spectra of both samples from Scotland (Fig. 2a) show a quartet of very intense bands in the 1500–1300 cm^{-1} range that are assigned, as discussed above, to the vibrations

of the carbonate CO_3 group. These bands are also present with very weak intensity in the spectra of all samples from Latium (Fig. 2b), and are virtually absent in the spectra of both samples from Vishnevy Gory (Fig. 2a). However, the interesting feature of Figure 2 is the sharp and prominent band at 2351 cm^{-1}, due to the presence of $^{12}CO_2$ molecules in most samples (cf. Khomenko and Langer 2005). It is prominent in both crystals from Vishnevy Gory, is absent in both specimens from Scotland and is present (although with reduced intensity) in all samples from Latium. Figure 3 displays the single-crystal spectrum in the MIR region of vishnevite V72 from Scotland, which can be compared to the spectrum of vishnevite from Urals given in Figure 1. It is apparent that both samples have very similar spectroscopic signals as regards the water absorptions; however, they are very different with respect to the C-O absorptions. The spectrum of vishnevite from Scotland shows very intense split bands in the CO_3 region, at 1505–1476 and 1406–1391 cm^{-1}, respectively. It also shows a quartet of well resolved weak bands at 2560–2530 and 2467–2440 cm^{-1}, respectively (arrowed in Fig. 3), which can be assigned to the combination of the ν_3 stretching modes of the CO_3 group at 1400–1500 cm^{-1} with a second mode of the CO_3 group around 1000 cm^{-1}, such as the ν_1 absorption at ~1085 cm^{-1} of the carbonate group in the aragonite configuration (White 1974). Note that in the transmission spectrum of the Scottish sample, a weak band due to CO_2 is also observed (Fig. 3); however its intensity is so low that this band disappears in the absorbance spectrum (Fig. 2a).

In summary, the information provided by the spectra of Figures 1 to 3 indicates that (1) all analyzed vishnevites contain CO_2 molecules in variable amounts, and (2) some samples contain CO_3 groups in addition to CO_2 molecules. In particular, vishnevite from Scotland contains almost all carbon in the form of CO_3 whereas vishnevite from the holotype locality Vishnevye Gory contains almost exclusively CO_2. All vishnevites from Latium contain systematically significant CO_2 with minor CO_3.

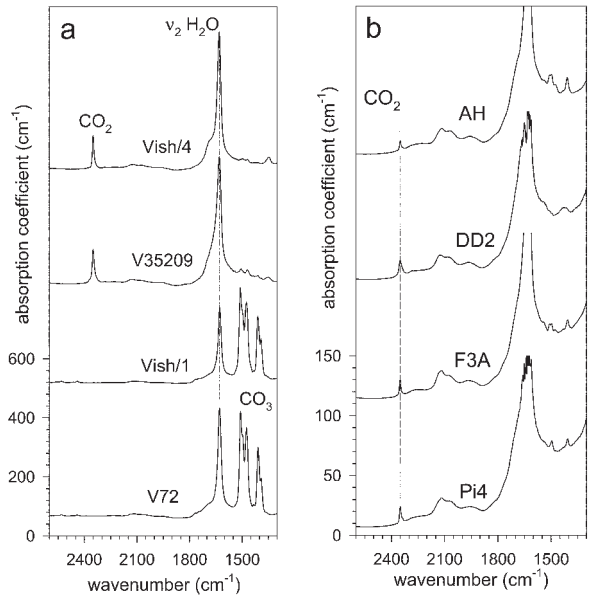

Figure 2. Unpolarized-light single-crystal FTIR spectra of vishnevites in the 2600–1300 cm^{-1} region for (**a**) vishnevites from Vishnevy Gory and Scotland and (**b**) vishnevites from Latium, Italy. For sample labels see Table 1. Absorbance normalized to thickness (*a* = A/t, in cm^{-1}); spectra offset for clarity.

The H-O bands

Unpolarized spectra of all vishnevite samples show typically a very complex fundamental H_2O stretching region consisting of (at least) two very intense and sharp bands at high frequency (3600–3500 cm^{-1}), plus a very broad, lower frequency absorption around 3300 cm^{-1}. The wavenumber of this latter absorption closely corresponds to the first overtone of the bending mode (2 ν_2) of the water molecule(s). It is systematically observed in the spectra of cancrinite-type minerals, however in all vishnevites its intensity is too high to be justified solely by the overtone of the bending mode, suggesting the overlap with an additional H_2O/OH absorption.

Refinement and description of the structure of vishnevite Pi4

The structure of sample Pi4 was refined in space group $P6_3$ starting from the atom coordinates of Hassan and Grundy (1984). In the early cycles, isotropic displacement factors were used and only the framework and the alkali cations in the structural pores were considered in the model. A total of five electron density maxima were identified in the difference-Fourier maps; one maximum located inside the cages was interpreted as an oxygen atom (since EMP analyses showed no Cl in the sample), and four maxima located inside the channel were assigned to one sulfur and three oxygen atoms, respectively, building-up a sulfate group in two possible orientations (up and down). These maxima were then added to the model; their coordinates were fixed to obtain reasonable S-O distances (see discussion later), and their site-occupancy and displacement parameters were refined as unconstrained. Significant positional disorder was observed for the alkali cations inside the channel, thus the site was split into two positions and refined with the scattering curves of K and

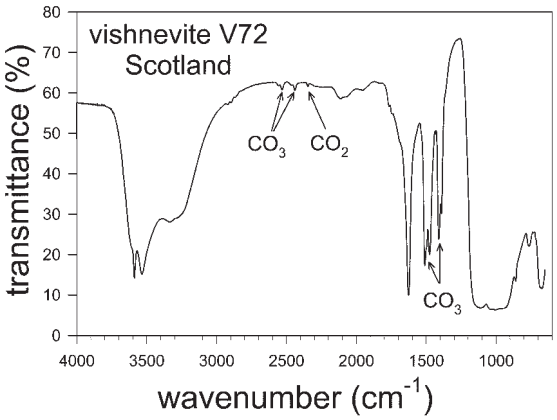

Figure 3. Single-crystal unpolarized-light spectrum of vishnevite V72 from Scotland in the MIR range.

TABLE 4. Atomic coordinates (×10⁴), equivalent isotropic displacement parameters and anisotropic displacement parameters (Å² × 10³) for vishnevite Pi4

Atom	Site	Occupancy	*x/a*1	*y/a*2	*z/c*	U_{iso}
Si	6c	1.0	834(1)	4134(1)	7562(8)	8(1)
Al	6c	1.0	3384(1)	4144(1)	7570(8)	9(1)
O1	6c	1.0	2019(1)	4044(1)	6799(9)	17(1)
O2	6c	1.0	1192(1)	5535(1)	7332(9)	23(1)
O3	6c	1.0	386(1)	3599(2)	419(9)	18(1)
O4	6c	1.0	3279(2)	3527(2)	597(9)	17(1)
S	2a	0.29	0	0	2918	45(2)
Na1	2b	0.83	⅔	⅓	1333(11)	34(1)
Na2	6c	0.35	1141(4)	2258(5)	2940(9)	24(1)
K2	6c	0.43	1458(3)	2894(4)	2893(9)	42(1)
O51	6c	0.22	615	1133	6725	150(20)
O52	6c	0.25	496	1090	9541	139(17)
O6	6c	0.33	6184	3043	6893	62(2)
O7	2a	0.22	0	0	737	68(8)
	U_{11}	U_{22}	U_{33}	U_{23}	U_{13}	U_{12}
Si	8(1)	9(1)	8(1)	1(1)	0(1)	5(1)
Al	9(1)	10(1)	8(1)	1(1)	0(1)	6(1)
O1	10(1)	26(1)	18(1)	0(1)	2(1)	11(1)
O2	22(1)	14(1)	35(1)	4(1)	6(1)	11(1)
O3	14(1)	27(1)	11(1)	4(1)	2(1)	11(1)
O4	21(1)	24(1)	11(1)	5(1)	−1(1)	15(1)
S	40(1)	40(1)	57(4)	0	0	20(1)
Na1	19(1)	19(1)	64(2)	0	0	10(1)
Na2	17(2)	39(3)	23(1)	−5(1)	−4(1)	20(2)
K2	38(1)	65(2)	32(1)	−6(1)	−3(1)	34(1)

Notes: U_{iso} is defined as one third of the trace of the orthogonalized U_{ij} tensor. The anisotropic displacement factor exponent takes the form: $-2\pi^2[h^2a^{*2}U_{11} + ... + 2\,h\,k\,a^*\,b^*\,U_{12}]$.

TABLE 5. Selected bond-distances (Å) and angles (°) for vishnevite Pi4

Framework atoms					
Si-O1	1.617(2)	O1-Si-O2	107.62(6)	Si-O1-Al	151.41(8)
Si-O2	1.608(2)	O1-Si-O3	109.93(8)	Si-O2-Al	148.56(9)
Si-O3	1.615(1)	O1-Si-O4	107.88(7)	Si-O3-Al	138.23(11)
Si-O4	1.620(2)	O2-Si-O3	112.35(10)	Si-O4-Al	138.29(11)
<Si-O>	1.615	O2-Si-O4	111.84(9)	<Si-O-Al>	144.12
V (Å³)	2.16	O3-Si-O4	107.14(7)		
TAV*	5.09	<O-Si-O>	109.46		
TQE*	1.0012				
Al-O1	1.724(2)	O1-Al-O2	106.13(6)		
Al-O2	1.722(2)	O1-Al-O3	107.44(7)		
Al-O3	1.747(2)	O1-Al-O4	109.32(8)		
Al-O4	1.733(2)	O2-Al-O3	113.82(9)		
<Al-O>	1.732	O2-Al-O4	114.15(9)		
V (Å³)	2.65	O3-Al-O4	106.05(6)		
TAV*	13.81	<O-Al-O>	109.49		
TQE*	1.0035				

Cage atoms		Channel atoms			
Na1-O1 ×3	2.900(1)	Na2-O1	2.810(5)	K2-O1	2.394(3)
Na1-O2 ×3	2.417(2)	Na2-O3	2.681(5)	K2-O3	2.354(3)
Na1-O6a	2.939(6)†	Na2-O3	3.020(5)	K2-O3	2.865(2)
Na1-O6b	2.369(6)†	Na2-O4	2.664(5)	K2-O4	2.361(3)
<Na1-O>	2.657	Na2-O4	3.002(5)	K2-O4	2.827(2)
		Na2-O51	2.326(5)	K2-O51	2.781(4)
(SO_4) groups		Na2-O51	2.297(5)	K2-O51	2.794(4)
		Na2-O51	2.193(5)	K2-O51	2.903(4)
S-O7	1.465†	Na2-O52	2.187(5)	K2-O52	2.644(4)
S-O51 ×3	1.395†	Na2-O52	2.375(5)	K2-O52	2.854(4)
<S-O>	1.430	Na2-O52	2.245(5)	K2-O52	2.982(4)
		Na2-O7	2.739(6)		
S-O7	1.134†	Na2-O7	2.882(6)		
S-O52 ×3	1.469†				
<S-O>	1.302				

Notes: TAV = tetrahedral angle variance; TQE = tetrahedral quadratic elongation.
* Robinson et al. (1971).
† Atoms fixed during the last cycles of refinement.

Na, respectively. The atomic displacement parameters were converted to the anisotropic form in the last cycles for all atoms but the oxygen atoms coordinating the sulfur and the oxygen atom within the cage; assuming a merohedral twinning [with (110) as twin law, refined twin fraction 0.494(3)], refinement converged to $R_{all} = 3.3\%$ and $wR^2 = 9.4\%$. Final coordinates and displacement parameters are reported in Table 4, selected bond distances and angles are given in Table 5 and observed and calculated structure factors are reported in Table 6[1].

The results of our refinement of vishnevite Pi4 from Latium are consistent with all other refinements of vishnevites and cancrinite-group minerals reported thus far (Grundy and Hassan1982; Hassan and Grundy 1984; Ballirano et al. 1998; Bonaccorsi et al. 1990; Ballirano and Maras 2004). In particular, the mean bond-lengths of the SiO_4 and AlO_4 tetrahedra confirm the presence of complete Al/Si order in the framework; the cancrinite cages (Fig. 4a) host sodium at the Na1 site that is planar coordinated by six oxygen atoms of the Al-Si framework at distances of 2.900(1) and 2.417(2) Å. Additionally there are two bonds to the oxygen atoms of the H_2O molecules at distances of 2.939(6) Å and 2.369(6) Å (Fig. 4a). These H_2O molecules probably have their O–H and H···H vectors lying within the (001) planes to avoid short Na···H distances. The observed site scattering at the Na1 site is $2 \times 0.83 \times 11$ e⁻ (Na) = 18.26 e⁻ (Table 4), which can be compared with 1.48 (which is Na apfu at the Na1 site after filling up the Na2 site with Na + K = 6.00) × 11 e⁻ (Na) + 0.05 × 20 e⁻ (Ca) + 0.01 × 26 e⁻ (Fe) = 17.54 e⁻ that we obtain from EMP analyses (Table 3).

The arrangement of cations and anion groups along the channels is complex. The Fourier-difference map projected onto (100), obtained by removing the O51, O52, and O7 sites from the model (Fig. 5), is consistent with a high degree of disorder. From the short S-S distances (2.60 Å) it turns out that any 2*a* position can only be half occupied by sulfur, hence the maximun number of (SO_4) groups in the structure is limited to 1 per formula unit (pfu). In addition, sites O7 and S can only be alternatively occupied (see Fig. 4c), hence, for one unit cell, the total scattering at these two sites must be ideally S (16 e⁻) + O (8 e⁻) = 24 e⁻ pfu. In contrast, the observed scattering at O7 and S is $2 \times 0.22 \times 8$ e⁻ + $2 \times 0.29 \times 16$ e⁻ = 12.8 e⁻ pfu (Table 4), which is significantly lower than the ideal value, and also lower than the amount of (SO_4) pfu measured by EMPA (Table 3). However, if we consider the basal oxygen atoms of the (SO_4) tetrahedron, we obtain $6 \times 0.22 \times 8$ e⁻ + $6 \times 0.25 \times 8$ e⁻ = 22.6 e⁻ pfu (Table 3), very close to the expected value (3×8 e⁻ = 24 e⁻) for 1 (SO_4) pfu, in agreement with the EMP data. Thus the strong deficiency in the observed scattering at the O7 and S positions may be explained by the high degree of disorder along

[1] Deposit item AM-07-018, Table 6 (observed and calculated structure factors). Deposit items are available two ways: For a paper copy contact the Business Office of the Mineralogical Society of America (see inside front cover of recent issue) for price information. For an electronic copy visit the MSA web site at http://www.minsocam.org, go to the American Mineralogist Contents, find the table of contents for the specific volume/issue wanted, and then click on the deposit link there.

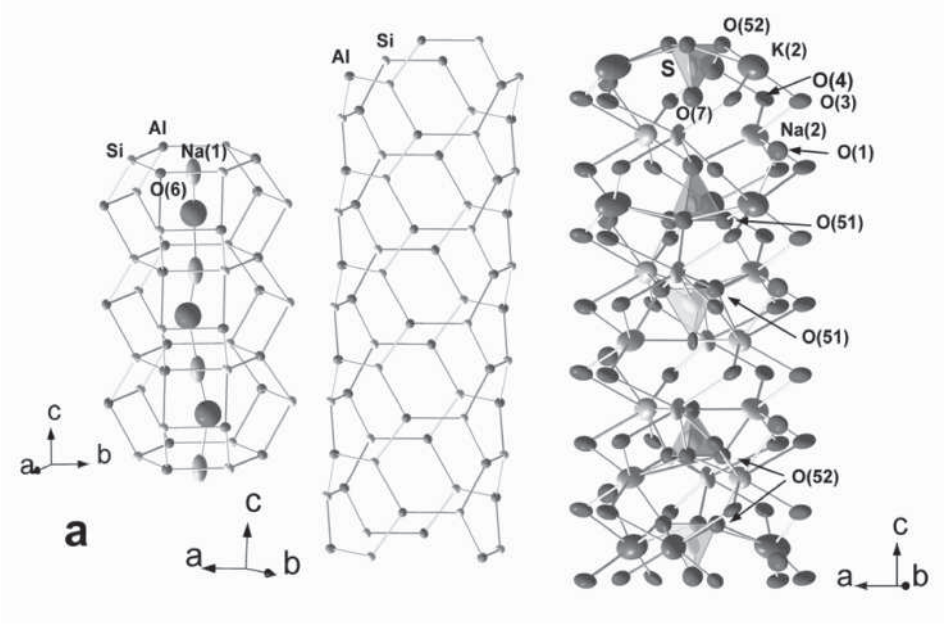

FIGURE 4. Sketch of (**a**) the cancrinite cages (showing the oxygen atoms of the H_2O groups bonded to the Na atoms at the Na1 sites), (**b**) the framework of the channel, and (**c**) a plausible sequence of ordering of (SO_4) groups along the channel showing several possible local coodination environments for the Na2 and K2 sites. Small white ellipsoids = Si atoms; small dark-gray ellipsoids = Al atoms; large dark-gray ellipsoids and spheres = O atoms; medium-gray large ellipsoids = K or Na at the K2 sites; light-gray large ellipsoids = Na atoms at the Na1 and Na2 sites; gray polyhedra = S atoms.

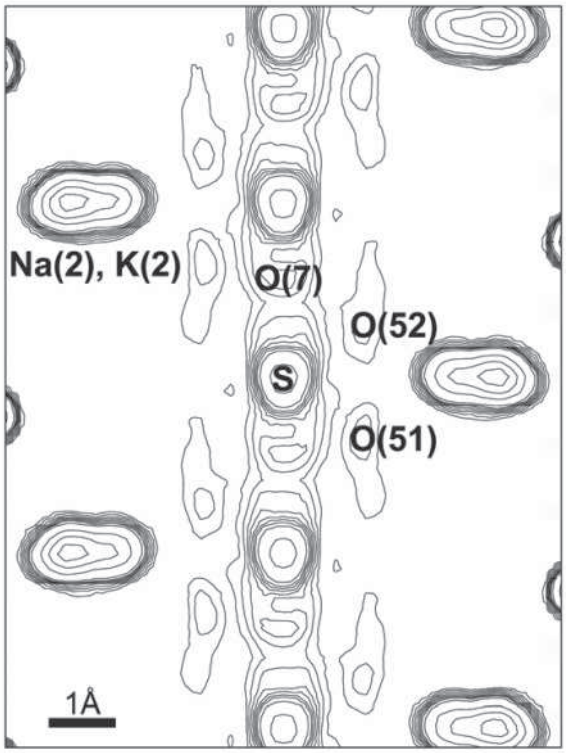

FIGURE 5. [$2F_o - F_c$] density map projected onto (100) obtained removing the O51, O52, and O7 oxygen atoms from the model. First contour at 1.5 $e^-Å^{-3}$. Contour steps of 0.5 $e^-Å^{-3}$ up to 5.5 $e^-Å^{-3}$. After that, contour steps of 5 $e^-Å^{-3}$ each.

the screw axis that makes it difficult to model completely the smeared electron density (Fig. 5).

The half occupation of the available sites for the (SO_4) groups along the channels also explains the splitting of the alkali positions within the channels: when the S or O7 positions are occupied, the alkalis are expected to move away from the 6_3 screw axis, to avoid short cation-cation distances. The Na2 site is closer to the 6_3 screw axis and the refined scattering corresponds to $6 \times 0.35 \times 11$ e^- (Na) = 23.1 e^- pfu, while the K2 site is farther and its site scattering is $6 \times 0.43 \times 19$ e^- (K) = 49 e^- pfu. The total observed scattering is thus 72.1 e^-, which is in excellent agreement with the value calculated from the formula reported in Table 3 [0.70×19 e^- (K) + 5.30×11 e^- (Na) = 71.6 e^- pfu]. In the disordered situation described above there are several possible local coordination environments for atoms at the Na2 and K2 sites (see Fig. 4c); as a consequence there are many possible average <Na2-O> and <K2-O> distances, thus we only list single distances in Table 5.

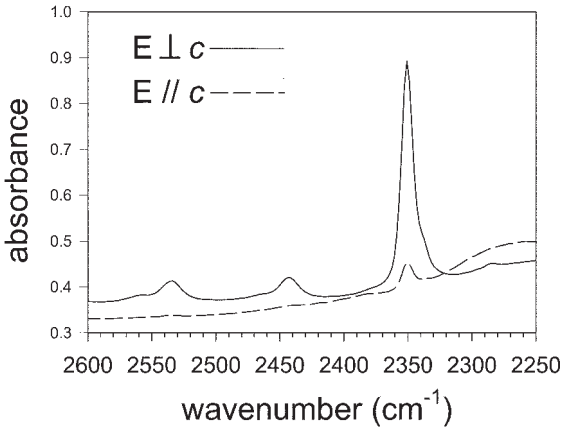

FIGURE 6. Polarized-light FTIR spectra of vishnevite Pi4 from Pitigliano, doubly polished section // **c**, thickness 150 μm.

On the basis of the structure refinement we propose the following crystal-chemical formula for the examined vishnevite sample: $[^{Na(2)}Na_{2.1}{}^{K(2)}(Na_{3.2}K_{0.7})(SO_4)_{1.01}][^{Na(1)}(Na_{1.66}Ca_{0.05}Fe_{0.01})(H_2O)_2][^{Si}Si_6{}^{Al}(Al_{5.76}Si_{0.24})O_{24}]$. In this formula Na at Na(1) site has been increased from 1.48 apfu to 1.66 to balance the 48 negative charges of the framework O atoms. However, besides channeling effects during EMP analyses that could be responsible for some depletion in alkali elements, resulting in totals <8 apfu, the above formula is also compatible with some vacancies at the alkali sites in the hexagonal-openings of the cancrinite-type cages. In this case, the charge deficit at O2 would be compensated via some substitution of Al by Si at the Al sites closer to the vacant Na1 site; in such a situation, the H_2O molecules inside the cage might be locally forced to rearrange themselves tilting their H···H and O-H vectors out of the (001) plane.

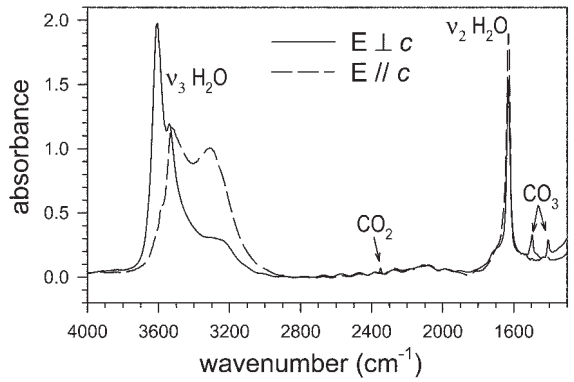

FIGURE 7. Polarized-light FTIR spectra of vishnevite Pi4 from Pitigliano, doubly polished section // **c**, thickness 40 μm.

Interestingly, we also observe that the density maxima of the oxygen sites inside the channel (Fig. 5) are blurred along the **c** axis, and this feature could be interpreted as H atoms attached to the oxygen atoms, in the form of OH or H_2O groups. In the latter case, the second H atom would point toward the center of the channel due to steric constraints, although it is not possible to confirm this case from the electron density map. The present refinement thus suggests the presence of H_2O/OH groups in the channels of vishnevite, in addition to those well known to be present in the cages.

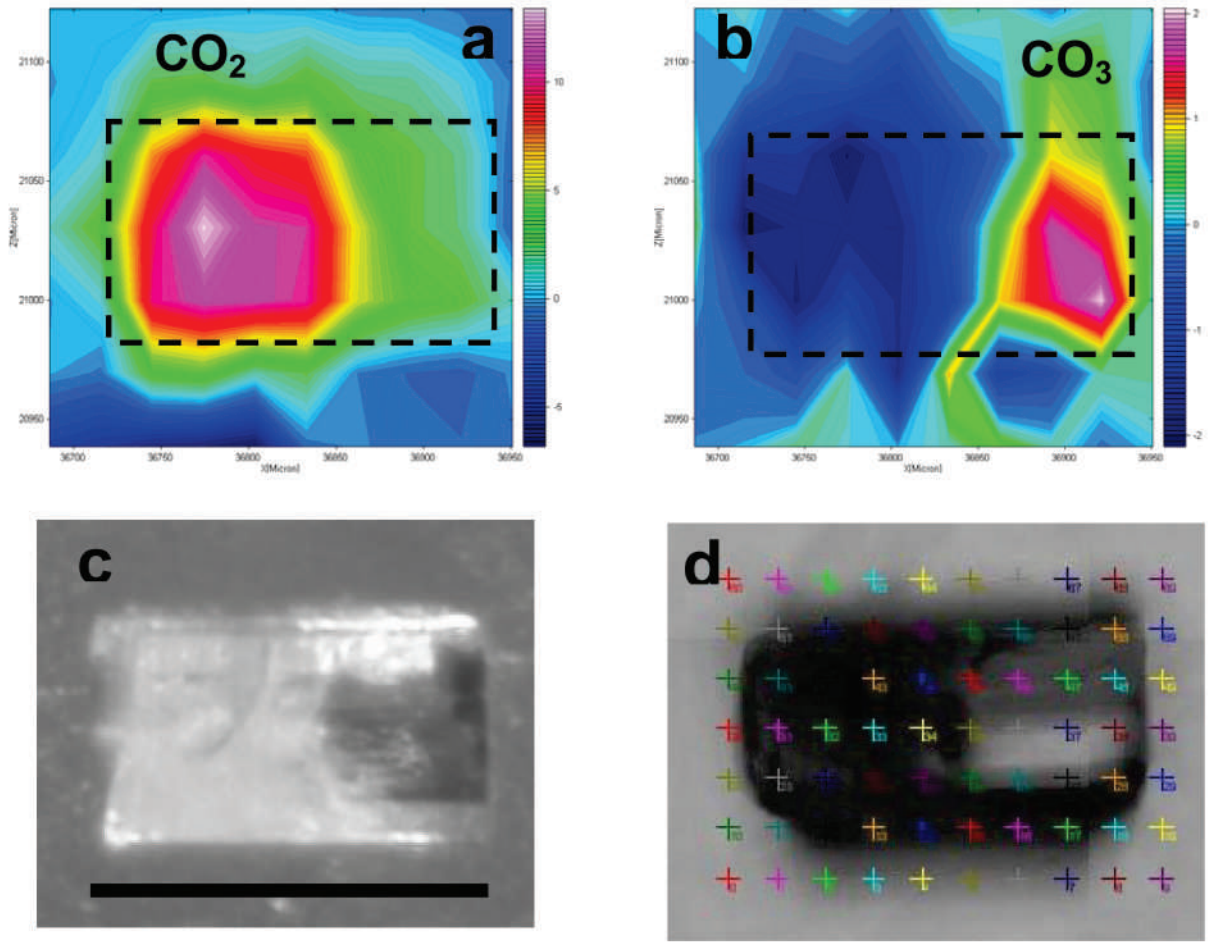

FIGURE 8. FTIR micro-spectroscopy mapping for CO_2 (**a**) and CO_3 (**b**) molecules (unpolarized-light spectra) across an optically zoned single crystal of vishnevite Pi4 from Pitigliano (**c**, the scale bar is 200 μm). The color scale from violet to blue is proportional to the intensity of the CO_2 (**a**) or CO_3 (**b**) bands. The broken-line box in **a** and **b** represents schematically the crystal area. (**d**) Shows the location of the analyzed spots.

Polarized-light FTIR spectra

Selected well-developed prismatic crystals of vishnevite Pi4 were doubly polished to variable thicknesses and oriented along [001] using the morphology as a guide. Figure 6 displays the spectra measured in the 2600–2250 cm^{-1} range on a thick (~150 μm) fragment with the electric vector **E**||**c** and **E**⊥**c**. Comparison of the two spectra shows that the CO_2 band at 2351 cm^{-1} is strongly polarized, with maximum integral absorption (A_{max} = 6.40 cm^{-1}) for **E**⊥**c** and a small residual intensity (A_{min} = 0.50 cm^{-1}) for **E**||**c**. This indicates that in vishnevite the structural CO_2 molecules are oriented perpendicular to the crystallographic **c** axis, like in pitiglianoite (Della Ventura et al. 2005) or in other microporous materials such as beryl (Wood and Nassau 1967) or cordierite (Armbruster and Bloss 1980; Aines and Rossman 1984). Note that the bands in the range 2400–2600 cm^{-1}, which have been assigned to the ($\nu_3 + \nu_1$) vibration of the CO_3 group (see above), are also polarized for **E**⊥**c** (Fig. 6); the same is observed for the stretching ν_{CO_3} modes in the 1500–1400 cm^{-1} range (see Fig. 7). Thus the FTIR data indicate that the planar carbonate CO_3 group is also oriented ⊥**c**, in agreement with X-ray diffraction structure refinement data on cancrinite-type minerals (Grundy and Hassan 1982; Ballirano et al. 1998; Ballirano and Maras 2004).

The water stretching region (3600–3200 cm^{-1}) was completely off-scale in the spectra discussed above, thus to study the polarization behavior of the H_2O bands a second crystal fragment had to be polished down to a thickness of ~40 μm. The spectra collected on this second fragment are displayed in Figure 7. Note that, due to the reduced thickness, the CO_2 band at 2350 cm^{-1} is barely visible, the principal CO_3 stretching bands at 1500–1400 cm^{-1} are very weak, and the CO_3 combination bands at 2550–2500 cm^{-1} have disappeared; the periodic noise in the 2800–2000 cm^{-1} region (interference fringes) is also due to the reduced sample thickness. Inspection of Figure 7 shows that the high-frequency band at ~3590 cm^{-1} is strongly polarized for **E**⊥**c**, while the intensity of the 3535 cm^{-1} component behaves almost isotropic. The broad band at ~3320 cm^{-1} is predominantly polarized for **E**||**c**; the bending mode at ~1630 cm^{-1} appears in both polarizations; however it is stronger for **E**||**c.**

Hydrogen in the structural pores of vishnevite

Interpretation of the spectra of Figure 7 is not straightforward; however when spectroscopic results are combined with X-ray refinement data and compared with recent studies (unpublished) on the closely related cancrinite, some conclusions can be drawn:

(1) The two stretching bands at 3590 and 3535 cm^{-1} are associated with a unique bending mode at 1630 cm^{-1}; this feature is compatible with a unique and asymmetric H-O-H water molecule in the sample. The polarized spectra show that the shorter H-O bond (higher frequency) in this water molecule is oriented ⊥**c**, whereas the longer O-H bond (lower frequency) is inclined with respect to **c**; in other words this H_2O group has its molecular plane tilted with respect the **c** axis. This situation is similar to what is observed in the FTIR spectrum of cancrinite where the same two stretching-band pattern is associated with a single bending mode. Preliminary neutron diffraction data (Redhammer, personal communication) show the presence of a unique type of strongly asymmetric water molecule in the structural cages. In this respect, it must be noted that previous work on a high-potassium vishnevite (X-ray refinement; Pushcharovskii et al. 1989) or on cancrinite [proton magnetic resonance (PMR); Sokolov et al. 1977] suggested the presence of two different water molecules with different crystallographic orientations in the examined samples. In our opinion, the present data can be interpreted on the basis of a simpler model with one type of H_2O. This water molecule can be identified, without any doubt, within the cages forming the well-known $H_2O\cdots Na\cdots H_2O$ sequence (see above).

(2) The X-ray single-crystal data collected here show some residual electron density within the channels (see above). Considering that there are no additional bending modes in the spectrum besides the band at 1630 cm^{-1} previously assigned to the water molecule within the cages, we interpret this electron density as OH. These OH-groups can be associated with the broad absorption at ~3320 cm^{-1}; this absorption is polarized predominantly for **E**||**c** (Fig. 7), in agreement with the orientation of the electron density observed in the Fourier maps (Fig. 5). An additional piece of evidence supporting the inferred presence of OH groups in the structural pores of the examined vishnevites is provided by the well-resolved doublet at 4080–3870 cm^{-1} (Fig. 1), which is also strongly polarized for **E**||**c**; as discussed above, several previous works (e.g., Stone and Walrafen, 1982; Ihinger et al. 1994) show that the 4080–3870 cm^{-1} bands can be assigned to O-H groups in the sample. This point is not a trivial one, since such absorptions are observed in most cancrinite-group minerals (unpublished) and thus a confident assignment of these bands to OH groups would imply that hydroxyls are much more common than previously believed in the structural pores of these materials.

Finally, an additional point to be discussed involves the presence of HCO_3 acid carbonate groups in the channels of vishnevite. HCO_3 groups have already been identified in natural (Galitskii et al. 1978) and synthetic (Gesing and Buhl 2000) cancrinite. In such a case, at least some of the additional H atoms detected by X-ray refinement within the channels could be associated with the few CO_3 groups locally substituting for SO_4 groups, which are detected by FTIR spectroscopy (Fig. 7).

It is obvious, however, from this work and from inspection of the data available in the literature, that further work is needed to clarify the exact location and speciation of H in the pores of cancrinite-group minerals, possibly by combining X-ray + neutron diffraction and spectroscopy.

Zoning of volatiles in vishnevite

A small prismatic crystal (~200 × 100 × 100 μm) of vishnevite Pi4 showing an evident zoning, from milky-white to transparent (Fig. 8c), was manually extracted from a myarolitic cavity of the host-rock and analyzed by FTIR using a Bruker Hyperion 3000 microscope equipped with a mapping stage and an LN_2 cooled MCT detector. The data were collected at a resolution of 4 cm^{-1} on an analytical grid that covered continuously the whole sample using a square aperture of 30 × 30 μm^2 (Fig. 8d); 150 spectra were averaged for each spectrum and 250 spectra were averaged for each background. In Figures 8a and 8b, the measured absorptions for CO_2 (band at 2351 cm^{-1}, Fig. 8a) and CO_3 (bands at 1300–1400 cm^{-1}, Fig. 8b) are mapped with their intensity proportional to the color scale from violet-red (high intensity) to blue (low intensity). It is apparent from Figures

8a and 8b that sample Pi4 is extremely compositionally zoned with respect to the carbon content: the side attached to the host rock (milky-white) is CO_3-free but is rich in CO_2, whereas the terminal part of the crystal (transparent) contains less CO_2 and is rich in CO_3. The same kind of results was obtained on a second sample from the Alban Hills region, showing the same difference as crystal Pi4. Recent high-*T* spectroscopic work shows that the extra-framework anionic composition of pitiglianoite, a cancrinite-type mineral very close to vishnevite, is strongly *T* dependent (Della Ventura et al. 2005), and our unpublished data show that vishnevite releases all CO_2 at $T > 500$ °C. This suggests that the CO_2 content of both pitiglianoite and vishnevite can be used as a geothermometer, and on this basis we can infer for vishnevite from Pitigliano a temperature of crystallization below 500 °C, in agreement with its occurrence as a late-stage, miarolitic cavity filling phase.

Acknowledgments

E. Caprilli, D. Di Domenico, and F.S. Stoppani kindly provided the studied samples from Latium. L. Touret (Paris) and O. Grubessi (Rome) allowed us to use the samples from the Museums of Paris and Rome, respectively. Thanks are due to Stefano Merlino (Pisa) and Annibale Mottana (Rome) for a critical reading of a preliminary draft of the manuscript. Constructive criticism by M. Gesing, E. Libowitzky, and an anonymous referee helped to improve the clarity of the manuscript. Financial support to GDV was provided by COFIN2005.

References cited

Aines, R.D. and Rossman, G.R. (1984) The high temperature behavior of water and carbon dioxide in cordierite and beryl. American Mineralogist, 69, 319–327.

Armbruster, T. and Bloss, F.D. (1980) Channel CO_2 in cordierites. Nature, 286, 140–141.

Ballirano, P. and Maras, A. (2004) The crystal structure of a "disordered" cancrinite. European Journal of Mineralogy, 16, 135–141.

Ballirano, P., Maras, A., Caminiti, R., and Sadun, C. (1995) Carbonate-cancrinite: in-situ real-time thermal processes studied by means of energy-dispersive X-ray powder-diffractometry. Powder Diffraction, 10, 173–177.

Ballirano, P., Maras, A., and Buseck, P.R. (1996) Crystal chemistry and IR spectroscopy of Cl- and SO_4-bearing cancrinite-like minerals. American Mineralogist, 81, 1003–1012.

Ballirano, P., Bonaccorsi, E., Merlino, S., and Maras, A. (1998) Carbonate groups in davyne: structural and crystal-chemical considerations. Canadian Mineralogist, 36, 1285–1292.

Beliankin, D.S. (1944) Vishnevite, and not sulphatic cancrinite. Dokladi Akademii Nauk USSR, 42, 304.

Bonaccorsi, E. and Merlino, S. (2005) Modular microporous minerals: Cancrinite-Davyne Group and C–S–H Phases. In G. Ferraris and S. Merlino, Eds., Micro- and Mesoporous Mineral Phases, p. 241–290. Reviews in Mineralogy and Geochemistry, Mineralogical Society of America, Chantilly, Virginia.

Bonaccorsi, E. and Orlandi, P. (1996) Second occurrence of pitiglianoite, a mineral of the cancrinite-group. Atti Società Toscana di Scienze Naturali, Memorie, Serie A, 103, 193–195.

Bonaccorsi, E., Merlino, S., and Pasero, M. (1990) Davyne: its structural relationships with cancrinite and vishnevite. Neues Jahrbuch für Mineralogie, Monatshefte, 1990, 97–112.

Cámara, F., Bellatreccia, F., Della Ventura, G., and Mottana, A. (2005) Farneseite, a new mineral of the cancrinite-sodalite group with a 14 layer stacking sequence. European Journal of Mineralogy, 17, 839–846.

Deer, W.A., Howie, R.A., and Zussman, J. (2004) Rock-Forming Minerals. Volume 4B. Framework Silicates, Silica Minerals, Feldspathoids and Zeolites (2nd ed.), 958 p. Geological Society, London.

Della Ventura, G. and Bellatreccia, F. (2004) The channel constituents of cancrinite-group minerals. Proceedings Micro- and Mesoporous Mineral Phases, Accademia Nazionale dei Lincei, 75–76. INFN, Frascati (Rome).

Della Ventura, G., Bellatreccia, F., and Bonaccorsi, E. (2005) CO_2 molecules in pitiglianoite, a mineral of the cancrinite-sodalite group. European Journal of Mineralogy, 17, 847–851.

Engelhardt, G., Felsche, J., and Sieger, P. (1992) The hydroxosodalite system $Na_{6+x}[SiAlO_4]_6(OH)_x$*$nH_2O$: formation, phase composition, and de- and rehydration studied by ^1H, ^{23}Na, and ^{29}Si MAS-NMR spectroscopy in tandem with thermal analysis, X-ray diffraction, and IR spectroscopy. Journal of American Chemical Society, 114, 1173–1182.

Galitskii, V.Yu., Grechushnikov, B.N., and Sokolov, Yu.A. (1978) Form of water in cancrinite. Russian Journal of Inorganic Chemistry, 23, 1749–1750.

Gesing, M. and Buhl, J.-Ch. (2000) Structure and spectroscopic properties of hydrogencarbonate containing alumosilicate sodalite and cancrinite. Zeitschrift für Kristallographie, 215, 413–418.

Grundy, H.D. and Hassan, I. (1982) The crystal structure of a carbonate-rich cancrinite. Canadian Mineralogist, 20, 239–251.

Hassan, I. and Grundy, H.D. (1984) The character of the cancrinite – vishnevite solid-solution series. Canadian Mineralogist, 22, 333–340.

——— (1991) The crystal structure of basic cancrinite, ideally $Na_8[Al_6Si_6O_{24}](OH)_2$*$3H_2O$. Canadian Mineralogist, 29, 377–383.

Khomenko, V.M. and Langer, K. (2005) Carbon oxides in cordierite channels: determination of CO_2 isotopic species and CO by single crystal IR spectroscopy. American Mineralogist, 90, 1913–1917.

King, P.L., Venneman, T.W., Holloway, J.R., Hervig, R.L., Lowenstern, J.B., and Forneris, J.F. (2002): Analytical techniques for volatiles: a case study using intermediate (andesitic) glasses. American Mineralogist, 87, 1077–1082.

Ihinger, P.D., Hervig, R.L., and McMillan. P.F. (1994) Analytical methods for volatiles in glasses. M.R. Carroll and J.R. Holloway, Eds., Volatiles in Magmas, 30, 67–121. Reviews in Mineralogy, Mineralogical Society of America, Chantilly, Virginia.

Merlino, S., Mellini, M., Bonaccorsi, E., Pasero, M., Leoni, L., and Orlandi, P. (1991) Pitiglianoite, a new feldspathoid from southern Tuscany, Italy: chemical composition and crystal structure. American Mineralogist, 76, 2003–2008.

Pouchou, J.L. and Pichoir, F. (1985) 'PAP' $\Phi(\rho Z)$ procedure for improved quantitative micro-analysis. In J.T. Armstrong, Ed., Microbeam Analysis, 104–160. San Francisco Press, California.

Pushcharovskii, D.Yu., Yamnova, N.A., and Khomyakov, A.P. (1989) Crystal structure of high-potassium vishnevite. Soviet Physics and Crystallography, 34, 37–39.

Robinson, K., Gibbs, G.V., and Ribbe, P.H. (1971) Quadratic elongation: A quantitative measure of distortion in coordination polyhedra. Science, 172, 567–570.

Sheldrick, G.M. (1996) SADABS, Siemens area detector absorption correction software. University of Göttingen, Germany.

Sokolov, Yu.A., Galitskii, V.Yu., Ilyukhin, V.V., Kobyakov, I.B., and Belov, N.V. (1977) Study of proton-containing groups in cancrinite by the PMR method. Soviet Physics and Crystallography, 22, 56–59.

Stone, J. and Walrafen, G.E. (1982) Overtone vibrations of OH groups in fused silica optical fibers. Journal of Chemical Physics, 76, 1712–1722.

White, W.B. (1974) The carbonate minerals. In V.C. Farmer Ed., The infrared spectra of Minerals, 227–284. The Mineralogical Society, London.

Wiebcke, M., Engelhardt, G., Felsche, J., Kempa, P.B., Sieger, P., Schefer, J., and Fischer, P. (1992) Orientational disorder of the hydrogen dihydroxide anion $O_2H_3^-$, in sodium hydroxosodalite dihydrate, $Na_8[Al_6Si_6O_{24}](OH)_2$*$2H_2O$: single-crystal X-ray and powder neutron diffraction and MAS NMR and FT IR spectroscopy. Journal of Physical Chemistry, 96, 392–397.

Wood, D.L. and Nassau, K. (1967) Infrared spetra of foreign molecules in beryl. The Journal of Chemical Physics, 47, 2220–2228.

Zhang, M., Wang, L., Hirai, S., Redfern, S.A.T., and Salje, E.K.D. (2005) Dehydroxylation and CO_2 incorporation in annealed mica (sericite): An infrared spectroscopic study. American Mineralogist, 90, 173–180.

Manuscript received December 22, 2005
Manuscript accepted December 20, 2006
Manuscript handled by Eugen Libowitzky